Journal of Cellular Biochemistry 91:808–820 (2004)

RGA Protein Associates With a TRPV Ion Channel During Biosynthesis and Trafficking

Jason C. Barnhill,[1] Alexander J. Stokes,[1] Murielle Koblan-Huberson,[1] Lori M.N. Shimoda,[1] Atsushi Muraguchi,[3] Chaker N. Adra,[4] and Helen Turner[2]*

[1]Laboratory of Cell Biology and Immunology, Queen's Center for Biomedical Research at The Queen's Medical Center, Honolulu, Hawaii
[2]Department of Cell and Molecular Biology, John A. Burns School of Medicine, University of Hawaii, Honolulu, Hawaii
[3]Department of Immunology, Faculty of Medicine, Toyama Medical and Pharmaceutical University, Toyama, Japan
[4]Department of Pathology, Beth Israel Deaconess Medical Center and Harvard Medical School, Boston, Massachusetts

Abstract TRPV ion channels transduce a range of temperature stimuli. We proposed that analysis of the protein–protein interactions made by TRPV2 might give insight into the key issues surrounding this channel. These issues include the potential functional significance of TRPV2 in non-sensory tissues, the molecules involved in transducing its activation signal(s) and the mechanism by which its trafficking to the cell surface is regulated. Here we describe the interaction of TRPV2 channel with the RGA gene product. RGA is a four-transmembrane domain, intracellularly localized protein. RGA associates with TRPV2 in a rat mast cell line that is a native context for both proteins. The interaction between TRPV2 and RGA is transient and occurs intracellularly. RGA does not accompany TRPV2 to the cell surface. Formation of the TRPV2/RGA complex is dependent upon a cellular glycosylation event, suggesting that RGA may play a chaperone or targeting role for TRPV2 during the maturation of the ion channel protein. These data record a novel protein–protein interaction for TRPV2 and provide a foundation for future study of the potential regulatory contribution of RGA to TRPV2 function. J. Cell. Biochem. 91: 808–820, 2004.

Key words: mast cells; calcium channels; vanilloid; MS4; heat

Ion channels of the transient receptor potential (TRP) family respond to diverse cellular stimuli [Minke and Cook, 2002; Montell et al., 2002], including variations across a physiological and pathophysiological temperature range. Temperature sensing is mediated by three members of the TRPV (vanilloid receptor-related) subfamily and by a TRPM (melastatin-related) channel with significant similarity to the TRPV proteins [Caterina et al., 1997, 1999; Clapham, 2002; Peier et al., 2002; Smith et al., 2002; Xu et al., 2002]. TRPV1 and TRPV2 (previously VR-1 and VRL-1) respond to heat in the pathophysiological range, being gated at 42 and 52°C, respectively. TRPV1 activity can be primed by accessory stimuli, such as acidified intracellular pH, ethanol, or the action of proalgesic cytokines. These accessory stimuli act to lower the threshold for responsiveness to temperature [Caterina et al., 1997; Jordt et al., 2000; Chuang et al., 2001; Olah et al., 2001; Trevisani et al., 2002]. TRPV1 contributes to direct temperature sensation and to the heightened sensation associated with tissue damage. To date no priming stimulus for TRPV2 has been identified. Moreover, while TRPV1 is understood as a target for intracellular second messengers (e.g., anandamide, ethanol) and signaling pathways that target Phospholipase

Jason C. Barnhill and Alexander J. Stokes contributed equally to this work.

Jason C. Barnhill's present address is Department of Chemistry, United States Military Academy, West Point, NY.

*Correspondence to: Helen Turner, PhD, University Tower 811, Queen's Medical Center, 1301 Punchbowl Street, Honolulu, HI 96813. USA. E-mail: hturner@queens.org

Received 12 September 2002; Accepted 14 January 2003
DOI 10.1002/jcb.10775

C [Smart et al., 2000; Chuang et al., 2001; Olah et al., 2001; Trevisani et al., 2002], the regulatory framework surrounding TRPV2 is poorly understood. Interestingly, the tissue distribution of TRPV2 extends beyond sensory neurons to non-excitable cell types including tissues of the immune system [Caterina et al., 1999; HT and AJS, unpublished observation]. The role and activation mechanism of TRPV2 in these non-sensory cells remains to be elucidated.

Various classes of ion channels are regulated by protein–protein interactions at a level that precedes their association with signaling complexes at the plasma membrane. Many channels are hetero-oligomers, with the pore-forming units associated with non-pore-forming accessory subunits [Green and Millar, 1995; MacKrill, 1999; Deutsch, 2002; Trimmer, 2002]. Accessory subunits often associate intracellularly with the channel proteins and accompany them to the cell surface. Diverse roles have been documented for these accessory proteins, including regulation of trafficking to the cell surface and interaction with regulatory second messengers or proteins that modulate channel gating or kinetics. Interestingly, a murine TRPV2 homolog, the GRC channel, displays regulated trafficking to the cell surface following growth factor stimulation of insulinoma cells [Kanzaki et al., 1999]. During the early stages of biosynthesis and trafficking, channels undergo complex processing in which intra-ER or Golgi-localized chaperones play an important role [Chang et al., 1997; Gothel and Marahiel, 1999; Deutsch, 2002]. Channels must maintain a complex topology, and oligomerization of the pore-forming units must proceed with an accuracy that guarantees absolute alignment of the selectivity filter region. Moreover, channel biogenesis may include post-translational modifications including multi-stage glycosylation, directed proteolysis and lipidation [Green and Millar, 1995; Petrecca et al., 1999; Kedei et al., 2001]. ER- and Golgi-resident accessory proteins assist in directing and maintaining the integrity of these processes.

We proposed that analysis of the protein–protein interactions made by TRPV2 might give insight into the key issues surrounding this channel. These issues include its potential functional significance in non-sensory tissues, the molecules involved in transducing its activation signal(s) and the mechanism by which its trafficking to the cell surface is regulated. Here we describe the interaction of the TRPV2 channel with a previously uncharacterized protein, the RGA (recombinase gene activator) gene product. RGA associates with TRPV2 in a rat mast cell line that is a native context for both proteins. This interaction occurs intracellularly. RGA does not appear to attain the cell surface in complex with TRPV2. Deglycosylation of cellular proteins results in a loss of interaction between TRPV2 and RGA. This loss correlates with the absence of a TRPV2 glycoform. Association with RGA is, therefore, a novel protein–protein interaction for TRPV2, and we propose that RGA may play a role in maturation or trafficking of TRPV2. Our data provide a foundation for future study of the potential regulatory contribution of RGA to TRPV2 function.

MATERIALS AND METHODS

Expression Constructs

Rat TRPV1 and TRPV2 cDNAs [Caterina et al., 1997, 1999] were sub-cloned into pcDNA4TO (Invitrogen, Carlsbad, CA) with primers that conferred an amino-terminal FLAG epitope tag. The C2.3 (RGA) cDNA [Tagoh et al., 1996] was subcloned into pcDNA5TO (Invitrogen) using primers that conferred a carboxy-terminal V5 epitope tag. The TRPV-C1 chimera was produced by a fusion PCR protocol and comprised the amino-terminal region of rat TRPV1 (residues 1–430) fused to the transmembrane and carboxy-terminal regions (residues 391–761) of rat TRPV2. The fused cDNA was subcloned into pcDNA4TO with the addition of a 5′ FLAG tag. All constructs were verified by sequencing.

Interaction Trap Analysis

The Cytotrap system (Stratagene, La Jolla, CA) was employed according to the manufacturer's instructions using a rat brain target library and baits produced by fusing the N-terminal cytoplasmic domain of rat TRPV1 or TRPV2 in frame at the C-terminus of hSos. The bait construct was verified by sequencing. Following yeast transformation and library screening, cDNAs from positive clones were isolated by PCR, gel-purified, and identified by sequencing using vector-specific primers. Sequences were processed using MacVector (Oxford Molecular) software, CLUSTALW and the NCBI and NPS BLAST alignment facilities.

Northern Analysis

Multiple tissue Northern membranes were from Clontech (Palo Alto, CA). Multiple cell line Northern blots were produced using 1 μg/lane poly A^+ mRNA isolated from the indicated cell lines via oligo-dT capture. Restriction digested cDNA probes were: TRPV2: 353 bp HincII/NotI; RGA: 665 bp KpnI/NotI. Probes were ^{32}P labeled using random priming. Membranes were hybridized with radiolabeled probe for 2 h/65°C. After two washes in 2× SSC/0.05% SDS/RT for 20 min and two washes in 0.1× SSC/0.1%SDS/50°C for 20 min, membranes were autoradiographed.

Mammalian Cell Culture and Stable Cell Line Generation

RBL2H3 cells and HEK293 cells stably transfected with the pcDNA6TR (Invitrogen) plasmid (encoding the tetracycline-sensitive TRex repressor protein) were maintained in DMEM with 10% fetal bovine serum (inactivated at 55°C for 1 h) supplemented with 2 mM glutamine. Cells were cultured in a humidified 5% CO_2 atmosphere at 37°C. Selection pressure on the TRex 293 cells was maintained using 10 μg/ml Blasticidin (Sigma, St. Louis, MO). For production of TRex HEK293 cells with inducible expression of either TRPV1, TRPV2, or TRPV-C1, parental cells were electroporated with each cDNA in pcDNA4TO and clonal cell lines were selected by limiting dilution in the presence of 400 μg/ml zeocin (Invitrogen). Stable cell TRPV2/RGA cell lines were produced by retransfection of HEK293-TRPV2 cells with pCDNA5TO-V5-RGA and selection in Zeocin (400 μg/ml) in combination with hygromycin (5 μg/ml). TRPV channel expression was induced using 1 μg/ml tetracycline for 16 h/37°C. Stable lines were screened for inducible protein expression using Western blot.

Lysis, Immunoprecipitation, and Western Blotting

Cells were pelleted (2,000*g*, 2 min) and washed once in ice cold PBS. Approximately 10^7 cells were lysed (ice, 30 min) in 350 μl of lysis buffer (50 mM HEPES pH 7.4, 75 mM NaCl, 20 mM NaF, 10 mM iodoacetamide, 0.5% (w/v) Triton X-100, 1 mM phenylmethylsulfonyl fluoride (PMSF), 500 μg/ml aprotinin, 1.0 mg/ml leupeptin, and 2.0 mg/ml chymostatin). Lysates were clarified (10,000*g*, 5 min). Supernatants were either mixed with 1.4 volumes acetone (−20°C for 1 h to pellet total protein) or tumbled (4°C for 2 h) with the indicated antibody. Acetone precipitates were harvested by centrifugation at 10,000*g* for 5 min. Immunocomplexes were captured using 15 μl Protein G-sepharose beads and washed twice in 1 ml lysis buffer. Samples were incubated (95°C for 8 min) in reducing SDS–PAGE buffer. Immunocomplexes were resolved by 10% SDS–PAGE in 25 mM Tris, 192 mM glycine, 0.05% (w/v) SDS, pH 8.8. Resolved proteins were electrotransferred to PVDF. For Western blotting, membranes were blocked using 5% non-fat milk/PBS/1 h/RT. Primary antibodies were dissolved in PBS/0.05% Tween-20/0.05% NaN_3 and incubated with membrane for 16 h at 4°C. Developing antibodies (anti-rabbit or anti-mouse IgGs conjugated to horseradish peroxidase) were diluted to 0.1 μg/ml in PBS/0.05% Tween-20 and incubated with membranes for 45 min at RT. Standard washes (4 × 5 min in 50 ml PBS/0.1% Tween-20 at RT) occurred between primary and secondary antibodies and following secondary antibody. Signal was visualized using ECL^+. Anti-FLAGM2 and anti-V5 were obtained from Sigma and Invitrogen, respectively.

Biotinylation of Immunocomplexes and Cell Surface Biotinylation

Immunoprecipitations were performed as above with the additional step of incubating washed immunocomplexes for 15 min at RT in 50 μl lysis buffer containing 1 mg/ml sulfo-NHS-biotin (Pierce Biotechnology, Rockford, IL) adjusted to pH 8.0. For cell surface biotinylation, intact cells were incubated (30 min at RT) with 1 mg/ml sulfo-NHS-biotin in PBS (pH 8.0). This procedure modifies the NH_2 groups of accessible external lysine residues. Cells were washed four times in PBS/25 mM NH_4Cl (to quench further biotinylation of internal proteins following lysis) and then lysed as above with the addition of 25 mM NH_4Cl to the lysis buffer. Biotinylated proteins were resolved by SDS–PAGE, transferred to PVDF, and visualized using streptavidin-HRP and ECL.

Immunofluorescence

Cells were fixed on glass coverslips (4% paraformaldehyde in PBS, 20 min, RT). Cells were permeabilized (0.4% Triton X-100 for 5 min at

RT). After blocking (0.2% Fish Skin Gelatin in PBS, 20 min, RT), coverslips were incubated with primary and secondary antibodies and the indicated stains ($DIOC_6$ 100 ng/ml for 5 min at RT; Hoecsht 33342 1 μg/ml for 2 min at RT (Molecular Probes, Eugene, OR)). Coverslips were washed four times in PBS between each stage of antibody exposure. After mounting, imaging was performed with an Olympus IX70 fluorescence inverted microscope with quadruple dichroic filter block and excitation filters (filter set 88000, Chroma, Rockingham, VT). F-view monochrome CCD camera, framegrabber and camera control software (Microsuite, Melville, NY) were from Soft Imaging Systems (Lakewood, CO). Z-series images were taken using a BioRad 1024 confocal connected to an Olympus IX70 microscope. Sections were taken at 0.5–2 μm intervals in the z-axis.

RESULTS

The Murine RGA Gene Product Interacts With the Amino-Terminal Cytoplasmic Tails of TRPV Ion Channels

We initiated a Sos-recruitment system (SRS) interaction trap analysis to identify proteins that interact with, and potentially regulate, TRPV ion channels. This yeast two-hybrid system has the advantages of readily identifiable false positive interactions (Ras-GTPase family members and their guanine-nucleotide exchange factors) and the potential for post-translational modification of bait and target in the cytosol [Aronheim and Karin, 2000]. Here, we describe the analysis of a cDNA clone isolated using the highly homologous amino-terminal cytoplasmic domains of TRPV1 and TRPV2 as baits to probe a cDNA library derived from rat brain. Sequencing and BLAST alignment of this cDNA clone identified it as corresponding to the mouse RGA gene product (Locus ID 19729, accession number NP033083.1, named as Recombinase Gene Activator) [Tagoh et al., 1996]. Murine RGA has also been defined as the rodent homolog of the *D. melanogaster* saliva (*slv*) gene product [Artero et al., 1998]. BLAST analysis yielded a proposed human homolog of the murine RGA protein (accession number NP061333). Figure 1A shows a ClustalW alignment of the murine and human RGA proteins, together with the translated product of the cDNA clone, VN12.1, isolated in our yeast two-hybrid screen.

The *RGA* gene encodes a 221 amino acid protein with four putative transmembrane domains, denoted by solid bars in Figure 1A. The protein sequence of RGA does not reveal any obvious protein–protein interaction or enzymatic domains, although RGA does contain sites for post-translational modification via N-linked glycosylation and phosphorylation. Topologically, RGA does not resemble the tetraspanins exemplified by CD9 and TAPA-1, lacking the large external loop separating the third and fourth transmembrane domains [Maecker et al., 1997]. Rather, RGA has topological similarity but limited sequence homology (<20%) to a disparate family of proteins recently classified as the MS4A superfamily, exemplified by the CD20 surface receptor and the HTm4 intracellular adapter protein [Liang et al., 2001; Liang and Tedder, 2001], and to the PRA1/2 intracellular trafficking proteins which fall outside of the MS4 family [Abdul-Ghani et al., 2001]. Figure 1B,C show a ClustalW alignment and phylogenetic trees generated using the protein sequences of murine and human RGA, and members of the MS4 family from both species. Genomic Blast analysis suggests that the murine *RGA* gene is located at chromosome 3E3, while the human version is at chromosome 1q21.

Our interaction trap analysis suggested that RGA might interact with the amino-termini of TRPV1 and/or TRPV2. We compared the expression patterns of the two genes using Northern blot. Figure 2A shows that both TRPV2 and RGA are widely expressed in the tissue and cell lines tested. A range of tissues express mRNA for both TRPV2 and RGA, including all of the primary immune system tissues examined. Both RGA and TRPV2 mRNAs are highly represented in the two mast cell lines examined, P815 and RBL2H3. Interestingly, neither TRPV2 mRNA nor protein (data not shown) were detected in the Ramos (B-lymphocyte) and Jurkat (T-lymphocyte) cell lines.

We sought to validate the potential interaction between RGA and TRPV channels at the protein level. Tetracycline-inducible expression systems for TRPV1, TRPV2, and RGA were created (Fig. 2B). In these systems, the ion channels TRPV1 and TRPV2 carry an N-terminal FLAG epitope tag, while the *RGA* gene carries a C-terminal V5 epitope tag. In co-immunoprecipitation experiments using these

expression systems, we noted a robust interaction between TRPV2 and RGA (Fig. 2C). In contrast, TRPV1 immunoprecipitates did not contain detectable RGA. On this basis, we hypothesized that the RGA/TRPV2 interaction was physiological, while the interaction trap of RGA via TRPV1 bait was a result of close homology between these two ion channels in the bait region. We produced a chimeric TRPV ion channel where the amino-terminal cytoplasmic tail of TRPV1 was fused to the transmembrane and carboxy-terminal regions of TRPV2. In-frame fusion of TRPV1 and TRPV2 was confirmed by cDNA sequencing. We verified the tetracycline-inducible production of a full-length TRPV-C1 protein by anti-FLAG Western blot. Immunofluorescent analysis suggested that the subcellular localization of TRPV2 and TRPV-C1 are similar (data not shown). We then asked if the TRPV-C1 protein associated with RGA. Figure 2D shows that detectable binding to RGA is lost when the TRPV1 amino-terminus region replaces the corresponding cytoplasmic tail of TRPV2. In control experiments, we noted that RGA does not interact with the hTRPc1 channel (data not shown). TRPc1, like TRPV1 and TRPV2, has several ankyrin repeat domains in its N-terminus.

We identified a rat mast cell line, RBL2H3, with endogenous expression of both TRPV2 and RGA (see Northern analysis in Fig. 2A). We sought to co-immunoprecipitate RGA and the endogenous TRPV2 ion channels in this cell context. The data in Figure 3A show that endogenous TRPV2 in the RBL2H3 mast cell line may be co-precipitated with V5-RGA. In the absence of an antibody raised against the endogenous RGA molecule, we asked if TRPV2 immunocomplexes isolated from non-transfected RBL2H3 contained a protein corresponding to the RGA molecular weight. Biotinylation of the anti-TRPV2 immunoprecipitates

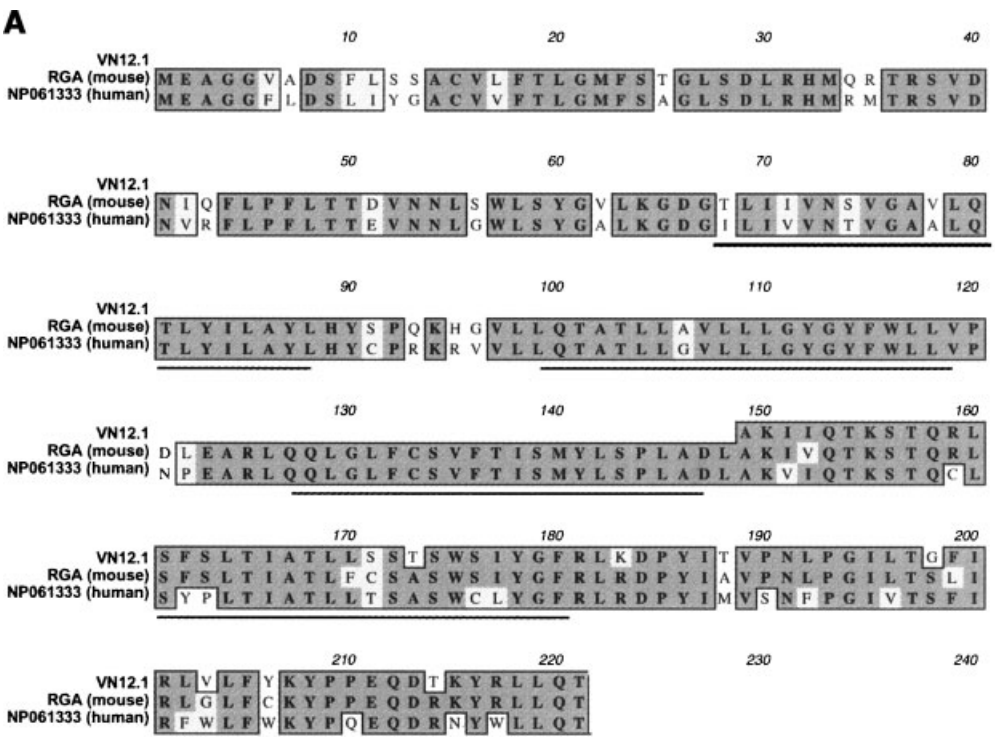

Fig. 1. **A**: ClustalW alignment of murine and human RGA proteins and cDNA clone isolated in yeast two hybrid screen. The VN12.1 clone was isolated from rat brain cDNA library and sequenced. Translation and BLAST alignment suggested that VN12.1 is a partial fragment corresponding to the murine RGA protein (accession number NP033083.1). BLAST alignment also revealed a human homolog of RGA, accession number NP061333. Solid lines indicate the putative transmembrane domains. **B**: ClustalW alignment of murine and human RGA proteins with MS4 family members. Amino acid sequences for MS4 family members and RGA proteins were loaded into MacVector software for ClustalW alignment on the basis of functional amino acid similarity. **C**: UPGMA (unweighted pair group method using arithmetic averages) analysis of murine and human MS4 and RGA protein sequences. Generated using MacVector on the basis of absolute similarity. Branch length correlates with sequence relatedness.

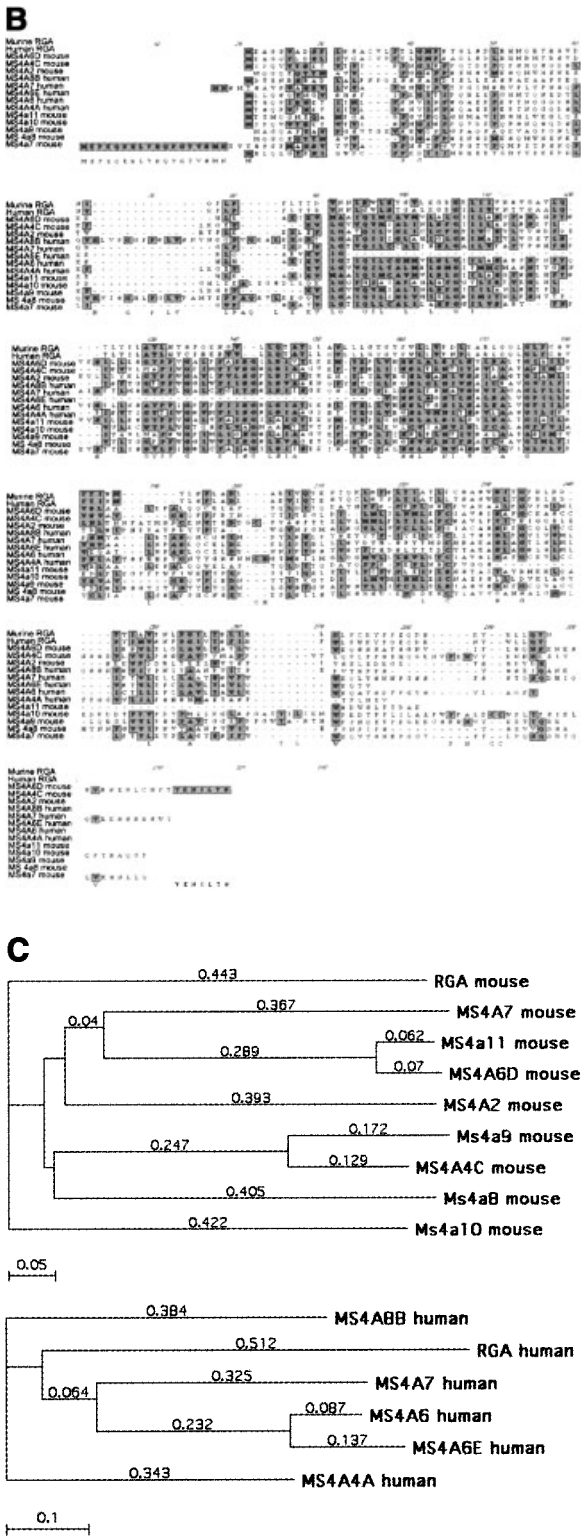

Fig. 1. (*Continued*)

revealed a 22 kDa protein that co-migrates with RGA in SDS–PAGE (Fig. 3B). Taken together, these data suggest that TRPV2 and RGA interact in this rat mast cell line.

RGA Is Located Intracellularly and Apparently Does Not Interact With TRPV2 at the Plasma Membrane

The function of RGA is presently unknown. We analyzed the subcellular localization of TRPV2 and RGA in the RBL2H3 cell system. Both TRPV2 and V5-RGA immunoreactivity can be seen in a compartment anchored over the nucleus in these cells (Fig. 4A), suggesting that this may be a region in which the proteins interact specific immunostaining for the endogenous TRPV2 molecules revealed both an intracellular population and an accumulation of channel molecules in a coronal pattern (Fig. 4A,B). This distribution is consistent with the likely intracellular trafficking and processing of TRPV2 en route to its destination in the plasma membrane. In contrast, RGA staining presented a solely intracellular pattern, consistent with localization in a compartment of the endoplasmic reticulum or Golgi apparatus (Fig. 4A, inset). Punctate or vesicular staining for RGA in the cytosol is consistent with the presence of an endosomal targeting motif in the carboxyl-terminus of the RGA protein. This motif, consisting of an acidic diad preceding a di-leucine motif (EXDXXXXLLXX), is an attractive target for future mutagenesis and resembles the endosomal retention motifs noted in the SUR accessory subunits involved in the trafficking of K_{ATP} ion channels [Sharma et al., 1999]. Similar data are obtained in HEK293 cells that stably express both TRPV2 and RGA (Fig. 4C).

On the basis of our immunofluorescence analysis, we proposed that the TRPV2 and RGA interaction occurs intracellularly and that RGA does not attain the cell surface in a complex with TRPV2. Indeed, while TRPV2 may be readily surface-biotinylated in intact cells, it is not possible to detect RGA by this method (Fig. 4D). The RGA molecule does contain several lysine residues in the regions that would form the putative extracellular loops (residues 88–99, residues 146–161). The observation that these lysines cannot be surface-biotinylated suggests that they are either masked while on the cell surface or are in fact intracellular.

RGA Association With TRPV2 Is Not Observed in Cells Treated With Tunicamycin

RBL2H3 mast cells are a native context for the TRPV2 protein. In this system, TRPV2 resolved by SDS–PAGE appears as a doublet. On the basis of previous studies by our group and published data on TRPV1 [Kedei et al., 2001], we propose that this doublet is likely to represent two glycoforms of TRPV2. TRPV2 contains two potential N-linked glycosylation sites, located in the extreme N-terminus and in the extracellular loop between transmembrane domains V and VI, at the mouth of the proposed pore. The RGA protein also has a single potential site for N-linked glycosylation in its amino-terminus. We asked if the N-glycosylation status of either TRPV2 or RGA influences the interaction between these two proteins. Figure 5 shows an immunoprecipitation experiment from cells treated, or not, with tunicamycin. This reagent blocks N-linked glycosylation at its earliest stage and prevents the addition of GlcNAc-PP-dolichol to asparagine residues

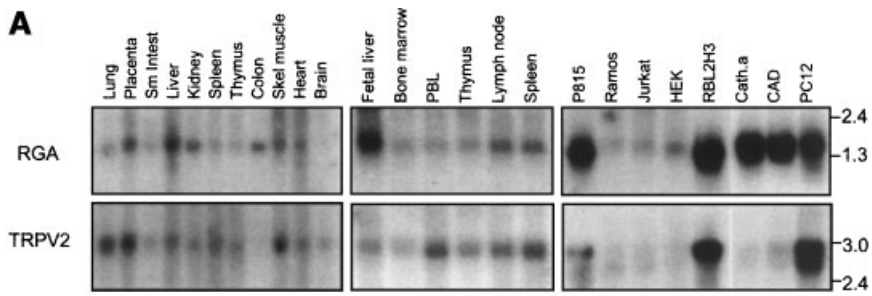

Tissue	RGA	TRPV2	Tissue	RGA	TRPV2
PBL	+	+	Fetal Liver	+	++
Lung	+	++	Bone marrow	+	++
Placenta	++	++	P815	++	+
Sm Intest	+	+	Ramos	+	-
Liver	++	+	Jurkat	+	-
Kidney	+	+	HEK	+	-
Spleen	+	+	RBL2H3	++	++
Thymus	+	+	Cath.a	++	-
Colon	+	-	CAD	++	-
Skel Musc	+	++	PC12	++	++
Heart	+	+			
Brain	-	+			

Fig. 2. **A**: Northern analysis of TRV2 and RGA mRNA expression. Multiple tissue Northern blots (**left panel**), multiple immune tissue (**center panel**) or multiple cell line Northern blots (**right panel**) were probed as described in Materials and Methods. Transcripts (1.4 and 2.7 kb) were hybridized using RGA and TRPV2 derived probes, respectively. PBL, peripheral blood leukocyte; P815, murine mast cell; Ramos, human B lymphocyte; Jurkat, human T lymphocyte; HEK, human embryonic kidney epithelium; RBL2H3, rat basophilic leukemia; Cath.a, murine catecholaminergic neuron; CAD, murine catecholaminergic neuron; PC12, rat phaeochromocytoma. Table summarizes observed expression patterns. **B**: Inducible expression of TRPV1, TRPV2, and RGA in HEK293 cells. Stable HEK293 cell lines transfected with *TRPV1*, *TRPV2*, or *RGA* genes under the control of an inducible promoter were produced as described in Materials and Methods. Cells (10^7 per lane) were treated with vehicle or with 1 μg/ml tetracycline for 16 h in order to induce gene expression. Cell lysates were immunoprecipitated with 2 μg anti-FLAGM2 or anti-V5 antibody per 10^7 cells and immunocomplexes were resolved by 10% SDS–PAGE. Resolved proteins were transferred to PVDF and immunoblots were probed with either anti-FLAG or anti-V5 antibodies. Note tetracycline-inducible expression of TRPV1 and TRPV2 proteins (97–99 kDa) and of V5-tagged RGA protein (21 kDa). **C**: Reciprocal immunoprecipitation of RGA proteins with TRPV2 ion channels. Stable HEK293 cell lines bearing the TRPV1 and TRPV2 cDNAs were transiently re-transfected with the pcDNA5TO plasmid containing V5-tagged RGA. Cells were treated for 16 h with tetracycline and lysates were prepared from 10^7 cells per lane. Lysates were immunoprecipitated as indicated with 2 μg anti-FLAGM2 or anti-V5 per 10^7 cells. After 10% SDS–PAGE, immunocomplexes were Western blotted for the presence of FLAG or V5-reactive proteins. Immunoprecipitates from TRPV2-expressing cells that were isolated using the V5 antibody contain both V5 and FLAG-reactive bands, indicating the presence of both RGA and TRPV2 proteins. Conversely, anti-FLAG immunoprecipitates from these cells contain a V5-reactive protein corresponding to RGA. **D**: Substitution of the TRPV2 amino-terminal cytoplasmic domain causes a loss of RGA binding. HEK293 were stably transfected with either TRPV2 or the TRPV-C1 chimera, and transiently re-transfected with the V5-RGA construct. Cells were treated for 16 h with tetracycline and lysates were prepared from 10^7 cells per lane. Lysates were immunoprecipitated as indicated with 2 μg anti-FLAGM2 antibody per 10^7 cells. After 10% SDS–PAGE, immunocomplexes were Western blotted for the presence of FLAG or V5-reactive proteins. Immunoprecipitates from TRPV2 expressing cells isolated using the V5 antibody contain both V5 and FLAG-reactive bands, indicating the presence of both RGA and TRPV2 proteins. TRPV-C1 immunocomplexes do not contain detectable RGA.

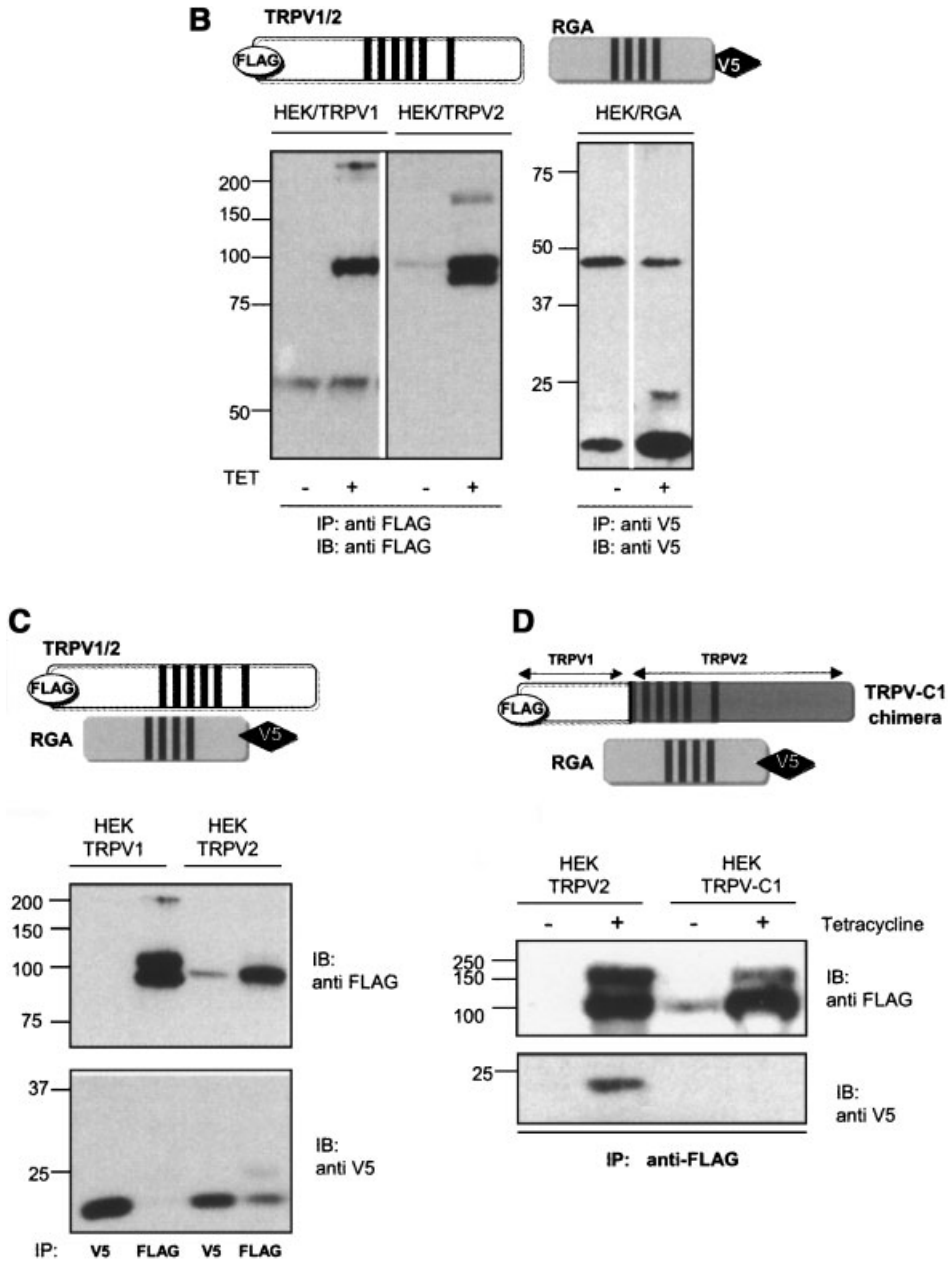

Fig. 2. (*Continued*)

[Elbein, 1987]. In samples derived from tunicamycin treated cells, the TRPV2 doublet is markedly reduced to a single, higher mobility (lower apparent molecular weight) band. Concomitant with the loss of the higher molecular weight form of TRPV2, we note that the RGA protein is no longer present in TRPV2 immunocomplexes isolated from tunicamycin treated cells. Thus the interaction between TRPV2 and the RGA protein depends, either directly or indirectly, upon a glycosylation event that is blocked by tunicamycin. RGA itself is apparently unaffected by tunicamycin treatment since the mobility of this protein in SDS–PAGE is identical in control and tunicamycin-treated cells (Fig. 5, lower panel). Lysates from RBL2H3 were also treated with either endoglycosidase H (endo H) or peptide *N*-glycosidase F (PNGase F). These reagents cleave high-mannose type and hybrid oligosaccharide chains, and a broad spectrum of N-linked sugars, respectively. In Endo H treated samples, the interaction between TRPV2 and V5-RGA was intact and we noted no alteration in TRPV2 or RGA mobility in 10%

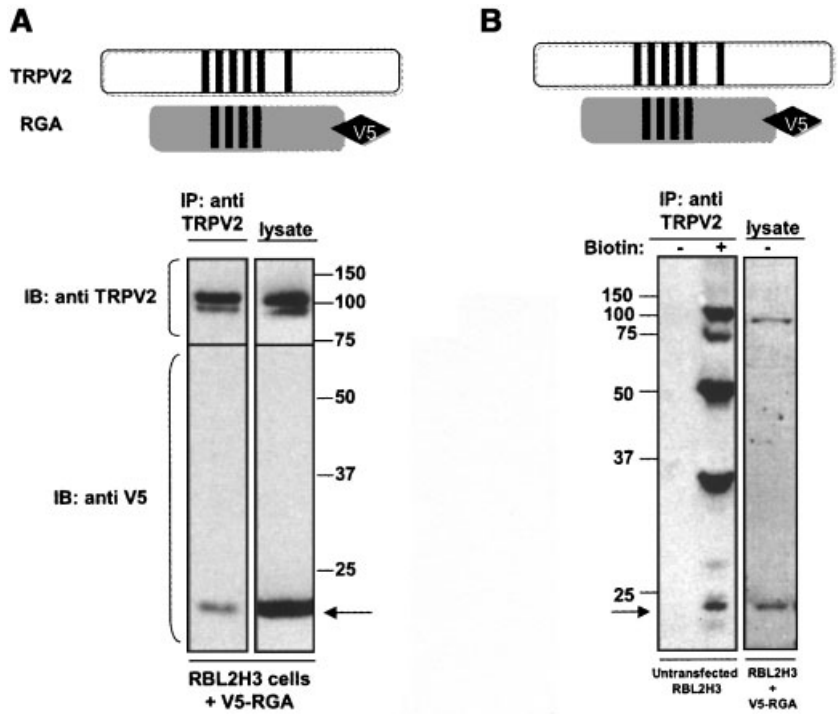

Fig. 3. **A**: Reciprocal immunoprecipitation of RGA proteins with endogenous TRPV2 ion channels in a mast cell line. RBL2H3 cells were transiently transfected with the pcDNA5TO containing V5-tagged RGA. After 16 h for recovery and protein expression, lysates were prepared (10^7 cells per lane) and immunoprecipitated as indicated with 11 μg anti-TRPV2 antibody per 10^7 cells (**left panel**) or acetone precipitated to recover total protein (**right panel**). After 10% SDS–PAGE, and transfer to PVDF, samples were Western blotted for TRPV2 or V5-reactive RGA protein. Note that immunoprecipitates from RBL2H3 cells isolated using the TRPV2 antibody contain both TRPV2 and the V5-tagged RGA protein. Arrow indicates V5-RGA band in total lysate. **B**: Endogenous TRPV2 immunocomplexes contain a protein that co-migrates with RGA. **Left panel**: Untransfected RBL2H3 (10^7 per lane) were immunoprecipitated with 7 μg anti-TRPV2 antibody per 10^7 cells. After two washes, immunocomplexes were biotinylated as described in Materials and Methods or left untreated. Protein complexes were resolved by 12.5% SDS–PAGE and transferred to PVDF. Protein bands were visualized using Streptavidin-HRP and ECL. Arrow marks 99 kDa TRPV2 and 21 kDa RGA proteins. The 50 and 26 kDa bands likely correspond to antibody heavy and light chains (data not shown). Identity of the 35 and 75 kDa bands is presently unknown. **Right panel**: Total lysate from RBL2H3 transfected with V5-RGA was resolved on a replicate 12.5% gel and transferred to PVDF. The membrane was probed with anti-V5 and protein bands were visualized using ECL. Arrow marks position of RGA protein.

SDS–PAGE (data not shown). PNGase F treatment caused loss of the upper (lower mobility) TRPV2 band in acetone-precipitated total lysates, and in replicate cell samples TRPV2 and RGA could not be co-precipitated (data not shown).

DISCUSSION

The TRPV2 ion channel has a documented role in the perception of extreme temperature elevations by cells. Its regulation and function in non-sensory cell contexts are not well understood. Here we document a novel protein interaction between TRPV2 and the RGA protein. This interaction was initially suggested by a yeast two-hybrid screen, and subsequently validated at the protein level by reciprocal co-immunoprecipitation. RGA is an intracellular protein that is localized to a vesicular subcompartment of the ER/Golgi apparatus. The interaction between RGA and TRPV2 is transient, since RGA does not accompany the channel subunits to the surface. The intracellular localization of RGA suggests that it is unlikely to play a highly specific role an as accessory molecule that confers gating or kinetic properties upon the pore-forming TRPV2 oligomer in the plasma membrane. Association between the two proteins is dependent on a cellular glycosylation event that is blocked by tunicamycin. In cells treated with tunicamycin, TRPV2 is apparently de-glycosylated, and this effect correlates with absence of RGA in TRPV immunocomplexes. Taken together, these data suggest that RGA is likely to function as a chaperone or

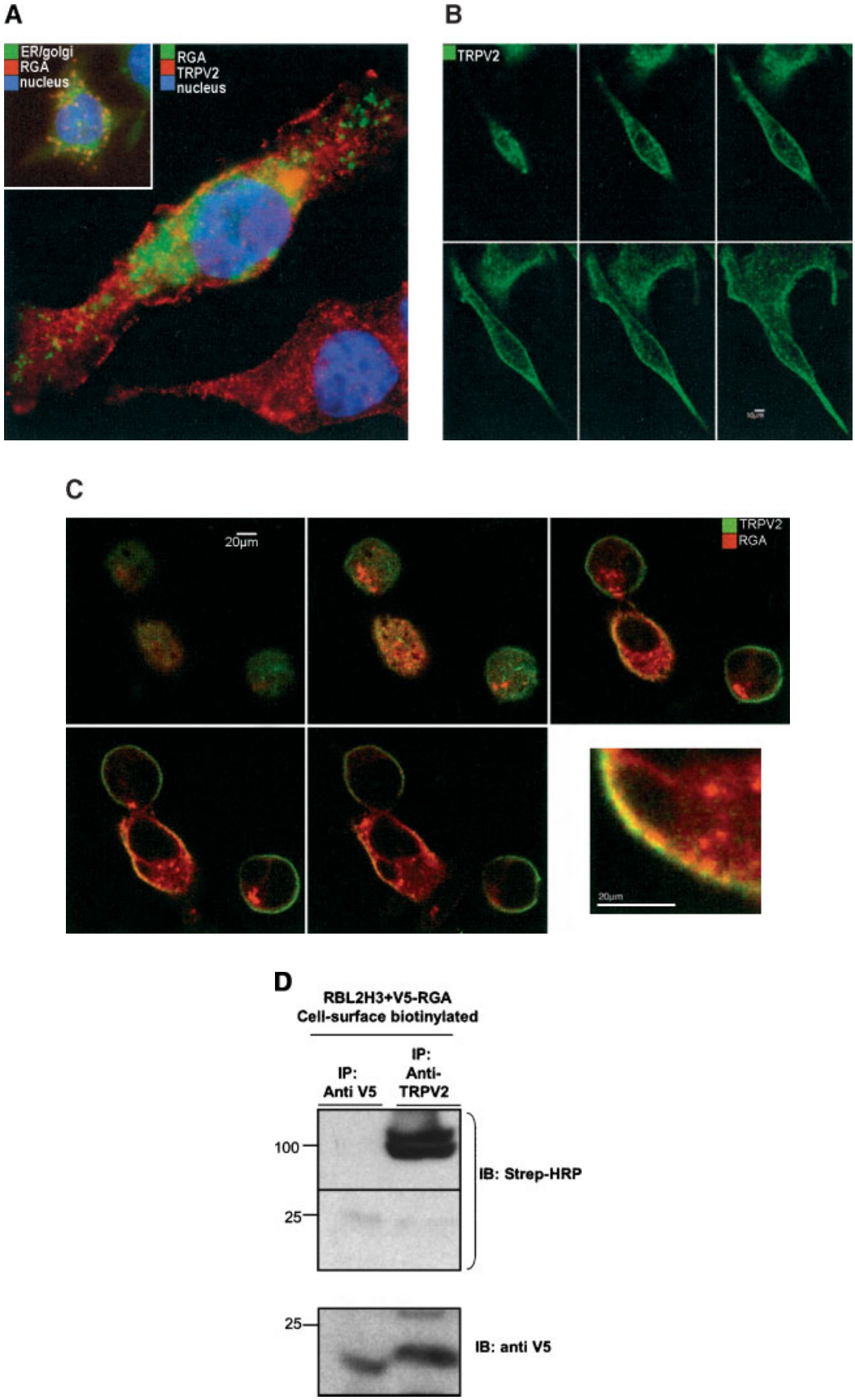
A
ER/golgi
RGA
nucleus
RGA
TRPV2
nucleus
B
TRPV2
C
20μm
TRPV2
RGA
20μm
D
RBL2H3+V5-RGA
Cell-surface biotinylated
IP:
Anti V5
IP:
Anti-
TRPV2
100
25
IB: Strep-HRP
25
IB: anti V5

Fig. 4.

targeting protein during channel maturation, rather than as a functional accessory subunit that is present in the pore-forming channel unit.

RGA and its homologs are proteins without defined molecular functions [Tagoh et al., 1996; Artero et al., 1998]. RGA was first identified when Tagoh et al. isolated the RGA cDNA from a B cell library during a screen for cDNAs whose products could induce expression of recombinase activating genes (RAG) in a murine B lymphocyte system [Tagoh et al., 1996]. There is no direct relationship between this finding and the data in the present report. However, a role in trafficking or the conformational chaperoning of a protein that can influence RAG transcription/translation can be inferred. These data raise the interesting question of whether RGA function is specific to TRPV2. We do not see an interaction between RGA and the closely related TRPV1 or hTRPC1 channels, suggesting that RGA is not a general regulator of TRP channel trafficking. It is conceivable that RGA is specific to TRPV2 in a given cell context, and resolution of this issue awaits further data on the protein–protein interactions made by RGA. In addition, the interaction between RGA and TRPV2 may not be direct, and we cannot yet state if an intermediary protein is involved.

The murine and human RGA proteins resemble MS4 proteins that are defined on the basis of a distinctive four-transmembrane topology, where short (~14 amino acid) loop regions separate the transmembrane domains [Liang and Tedder, 2001]. The genes for several members of MS4 group cluster at chromosomes 19D and 11q12-q13.1 in the mouse and human, respectively, [Liang et al., 2001]. *RGA* genes fall outside of these regions, as do two of the six known human *MS4* genes and several of the murine *MS4* genes [Liang and Tedder, 2001]. Absolute sequence homology between RGA and MS4 proteins is low. However, MS4 proteins are disparate, and aside from the low complexity transmembrane regions, MS4 family members have overall low sequence homology and are structurally diverse in their amino- and carboxyl-termini.

It is not yet known if MS4 family proteins can be grouped on the basis of analogous functionality. While few MS4 proteins have assigned functions, the marked diversity in the known roles of these proteins attests to the utility of the four-transmembrane topology in many biological processes. MS4 proteins with assigned roles comprise the following: HTm4 is an intracellular adapter protein that binds the KAP phosphatase and is involved in cell cycle regulation in hematopoietic cells [Donato et al., 2002]. CD20 and the FcεRI beta chain are cell surface proteins. The latter forms a signaling subunit of the high affinity receptor for immunoglobulin E, an antigen receptor that drives

Fig. 4. (*Overleaf*) **A**: Intracellular localization of TRPV2 and RGA proteins in RBL2H3 cells. RBL2H3 cells were transiently transfected with pcDNA5TO containing V5-RGA and seeded onto coverslips. Immunofluorescent detection of V5-RGA and TRPV2 was performed using 2 μg/ml anti-TRPV2 or anti-V5 specific primary antibodies and Alexa 488 or Alexa 568-conjugated secondary antibodies as described in Materials and Methods. **Main panel**: Anti-TRPV2 (red), anti-V5 (green), and Hoechst 33342 (blue) staining of RBL2H3 transfected with V5-RGA. Note punctate vesicular structures containing RGA protein. Endogenous TRPV2 is present in intracellular and plasma membrane locations. Both proteins localize to a prominent compartment above the nucleus (orange signal). Adjacent untransfected cell shows only anti-TRPV2 reactivity. Inset: RGA immunoreactivity is located within a subset of the ER/Golgi compartment. Live-cell staining with $DiOC_6$ (green) was used to delineate ER/golgi membranes. Cells were co-stained for V5-RGA (red) and the nucleus (blue). Replicate coverslips stained with secondary antibody alone displayed a negligible background contribution (data not shown). **B**: Confocal series of RBL2H3 cells immunostained for localization of TRPV2. RBL2H3 were seeded onto glass coverslips and stained using anti-TRPV2 and an Alexa-488 conjugated secondary antibody. A z-series was captured using a BioRad 1024 confocal microscope system. The vertical range of the image series was 20 μm. The cell surface is shown in the **upper left panel**, and the series progresses towards the plane in which the cell adheres to the coverslip (**lower right panel**). The scale bar measures 10 μm. **C**: Confocal series of HEK293 cells immunostained for localization of TRPV2 and V5-RGA. HEK293 were stably transfected with both FLAG-TRPV2 and V5-RGA constructs. Immunofluorescent detection of V5-RGA and TRPV2 was performed using 2 μg/ml anti-TRPV2 or anti-V5 specific primary antibodies and Alexa-488 or Alexa-568 conjugated secondary antibodies. The vertical range of the image series is 20 μm. The cell surface is shown in the **upper left panel**, and the series progresses towards the plane in which the cell adheres to the coverslip (**lower center panel**). **Lower right panel** shows a 5× expanded view of the plasma membrane region of a cell co-expressing TRPV2 and RGA. Scale bars measure 20 μm. **D**: Surface biotinylation of RBL2H3 cells expressing TRPV2 and V5-RGA. RBL2H3 cells were transiently transfected with the pcDNA5TO plasmid containing V5-tagged RGA. After 16 h for recovery and protein expression, cells were treated for 30 min at 37°C with 25 μM forskolin to induce surface translocation of TRPV2 (manuscript in preparation). Intact cells (1×10^7) were washed and cell-surface proteins with exposed lysine residues were biotinylated. After quenching, lysis and immunoprecipitation was performed as above using either 11 μg anti-TRPV2 or 3 μg anti-V5. Immunocomplexes were resolved on duplicate 10% SDS–PAGE gels. Following transfer to PVDF, one membrane was probed with Streptavidin-HRP (**top panels**) and the other was probed with V5 antibody (**lower panel**).

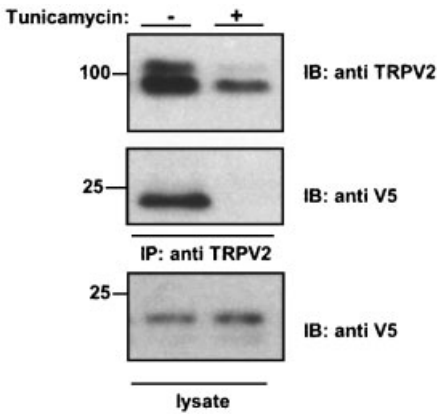

Fig. 5. The interaction between TRPV2 and V5-RAG is disrupted in tunicamycin-treated cells. RBL2H3 cells were transiently transfected with the pcDNA5TO plasmid containing V5-tagged RGA. During a 16 h recovery period, cells were exposed to either vehicle or 5 μg/ml tunicamycin as indicated. Immunoprecipitation of endogenous TRPV2 or V5-RGA was performed as above and total lysate was produced from the same cell samples to control for expression of V5-RGA. Protein samples were resolved by SDS–PAGE and Western blotted using the indicated antibodies.

the pro-inflammatory responses of mast cells and basophils [Turner and Kinet, 1999; Donnadieu et al., 2000]. CD20 is expressed exclusively in B-lymphocytes. CD20 is important clinically, since anti-CD20 (Rituximab) is a successful therapeutic agent in B-lymphoma [Grillo-Lopez et al., 2002]. Functionally, CD20 has been proposed to be an ion channel subunit, since over-expression of CD20 confers a calcium conductance upon heterologous cell systems [Kanzaki et al., 1995, 1997]. However, CD20 does not have any of the structural features associated with the pore-forming subunits of known calcium-selective cation channels. The interaction between RGA and TRPV2 raises the intriguing possibility that an analogous role for CD20 in trafficking of a B cell ion channel could contribute to the apparent conductance attributed to CD20 itself.

The data presented here represent the first potentially regulatory interaction demonstrated for the TRPV2 ion channel. Future experiments will be directed towards analysis of the extent to which RGA expression and interaction can influence TRPV2 surface trafficking and function. Biochemical evaluation of endogenous RGA awaits the ongoing development of specific antiserum to this protein. Moreover, conclusions as to the exact subcellular localization of endogenous RGA will also depend on this reagent. The relationship between RGA interaction and the glycosylation status of TRPV2 is of particular interest. TRPV2 has a complex glycosylation pattern, as does TRPV1 [Kedei et al., 2001]. It is not yet clear how glycosylation status influences TRPV channel behavior, but this is a clear candidate for a regulatory effect by RGA. In addition, the potential for topologically similar MS4 proteins to influence ion channel trafficking suggests a novel direction for research on this extensive protein family.

ACKNOWLEDGMENTS

The authors gratefully acknowledge the support of the Queen Emma Research Foundation and staff of Queens Medical Center. L. Doescher provided excellent technical assistance. Dr. David Julius (UCSF) generously provided TRPV1 and TRPV2 cDNAs.

REFERENCES

Abdul-Ghani M, Gougeon PY, Prosser DC, Da-Silva LF, Ngsee JK. 2001. PRA isoforms are targeted to distinct membrane compartments. J Biol Chem 276:6225–6233.

Aronheim A, Karin M. 2000. Analysis and identification of protein–protein interactions using protein recruitment systems. Methods Enzymol 328:47–59.

Artero RD, Terol-Alcayde J, Paricio N, Ring J, Bargues M, Torres A, Perez-Alonso M. 1998. Saliva, a new *Drosophila* gene expressed in the embryonic salivary glands with homologues in plants and vertebrates. Mech Dev 75:159–162.

Caterina MJ, Schumacher MA, Tominaga M, Rosen TA, Levine JD, Julius D. 1997. The capsaicin receptor: A heat-activated ion channel in the pain pathway. Nature 389:816–824.

Caterina MJ, Rosen TA, Tominaga M, Brake AJ, Julius D. 1999. A capsaicin-receptor homologue with a high threshold for noxious heat. Nature 398:436–441.

Chang W, Gelman MS, Prives JM. 1997. Calnexin-dependent enhancement of nicotinic acetylcholine receptor assembly and surface expression. J Biol Chem 272: 28925–28932.

Chuang HH, Prescott ED, Kong H, Shields S, Jordt SE, Basbaum AI, Chao MV, Julius D. 2001. Bradykinin and nerve growth factor release the capsaicin receptor from PtdIns(4,5)P2-mediated inhibition. Nature 411: 957–962.

Clapham DE. 2002. Signal transduction. Hot and cold TRP ion channels. Science 295:2228–2229.

Deutsch C. 2002. Potassium channel ontogeny. Annu Rev Physiol 64:19–46.

Donato JL, Ko J, Kutok JL, Cheng T, Shirakawa T, Mao XQ, Beach D, Scadden DT, Sayegh MH, Adra CN. 2002. Human HTm4 is a hematopoietic cell cycle regulator. J Clin Invest 109:51–58.

Donnadieu E, Jouvin MH, Kinet JP. 2000. A second amplifier function for the allergy-associated Fc(epsilon)RI-beta subunit. Immunity 12:515–523.

Elbein AD. 1987. Inhibitors of the biosynthesis and processing of N-linked oligosaccharide chains. Annu Rev Biochem 56:497–534.

Gothel SF, Marahiel MA. 1999. Peptidyl-prolyl *cis–trans* isomerases, a superfamily of ubiquitous folding catalysts. Cell Mol Life Sci 55:423–436.

Green WN, Millar NS. 1995. Ion-channel assembly. Trends Neurosci 18:280–287.

Grillo-Lopez AJ, Hedrick E, Rashford M, Benyunes M. 2002. Rituximab: Ongoing and future clinical development. Semin Oncol 29:105–112.

Jordt SE, Tominaga M, Julius D. 2000. Acid potentiation of the capsaicin receptor determined by a key extracellular site. Proc Natl Acad Sci USA 97:8134–8139.

Kanzaki M, Shibata H, Mogami H, Kojima I. 1995. Expression of calcium-permeable cation channel CD20 accelerates progression through the G_1 phase in Balb/c 3T3 cells. J Biol Chem 270:13099–13104.

Kanzaki M, Lindorfer MA, Garrison JC, Kojima I. 1997. Activation of the calcium-permeable cation channel CD20 by alpha subunits of the Gi protein. J Biol Chem 272:14733–14739.

Kanzaki M, Zhang YQ, Mashima H, Li L, Shibata H, Kojima I. 1999. Translocation of a calcium-permeable cation channel induced by insulin-like growth factor-I. Nat Cell Biol 1:165–170.

Kedei N, Szabo T, Lile JD, Treanor JJ, Olah Z, Iadarola MJ, Blumberg PM. 2001. Analysis of the native quaternary structure of vanilloid receptor 1. J Biol Chem 276:28613–28619.

Liang Y, Tedder TF. 2001. Identification of a CD20-, FcepsilonRIbeta-, and HTm4-related gene family: Sixteen new MS4A family members expressed in human and mouse. Genomics 72:119–127.

Liang Y, Buckley TR, Tu L, Langdon SD, Tedder TF. 2001. Structural organization of the human *MS4A* gene cluster on chromosome 11q12. Immunogenetics 53:357–368.

MacKrill JJ. 1999. Protein–protein interactions in intracellular Ca^{2+}-release channel function. Biochem J 337: 345–361.

Maecker HT, Todd SC, Levy S. 1997. The tetraspanin superfamily: Molecular facilitators. FASEB J 11:428–442.

Minke B, Cook B. 2002. TRP channel proteins and signal transduction. Physiol Rev 82:429–472.

Montell C, Birnbaumer L, Flockerzi V. 2002. The TRP channels, a remarkably functional family. Cell 108: 595–598.

Olah Z, Karai L, Iadarola MJ. 2001. Anandamide activates vanilloid receptor 1 (VR1) at acidic pH in dorsal root ganglia neurons and cells ectopically expressing VR1. J Biol Chem 276:31163–31170.

Peier AM, Reeve AJ, Andersson DA, Moqrich A, Earley TJ, Hergarden AC, Story GM, Colley S, Hogenesch JB, McIntyre P, Bevan S, Patapoutian A. 2002. A heat-sensitive TRP channel expressed in keratinocytes. Science 296:2046–2049.

Petrecca K, Atanasiu R, Akhavan A, Shrier A. 1999. N-linked glycosylation sites determine HERG channel surface membrane expression. J Physiol 515:41–48.

Sharma N, Crane A, Clement JPt, Gonzalez G, Babenko AP, Bryan J, Aguilar-Bryan L. 1999. The C terminus of SUR1 is required for trafficking of KATP channels. J Biol Chem 274:20628–20632.

Smart D, Gunthorpe MJ, Jerman JC, Nasir S, Gray J, Muir AI, Chambers JK, Randall AD, Davis JB. 2000. The endogenous lipid anandamide is a full agonist at the human vanilloid receptor (hVR1). Br J Pharmacol 129:227–230.

Smith GD, Gunthorpe MJ, Kelsell RE, Hayes PD, Reilly P, Facer P, Wright JE, Jerman JC, Walhin JP, Ooi L, Egerton J, Charles KJ, Smart D, Randall AD, Anand P, Davis JB. 2002. TRPV3 is a temperature-sensitive vanilloid receptor-like protein. Nature 418:186–190.

Tagoh H, Kishi H, Muraguchi A. 1996. Molecular cloning and characterization of a novel stromal cell-derived cDNA encoding a protein that facilitates gene activation of recombination activating gene (*RAG*)-1 in human lymphoid progenitors. Biochem Biophys Res Commun 221:744–749.

Trevisani M, Smart D, Gunthorpe MJ, Tognetto M, Barbieri M, Campi B, Amadesi S, Gray J, Jerman JC, Brough SJ, Owen D, Smith GD, Randall AD, Harrison S, Bianchi A, Davis JB, Geppetti P. 2002. Ethanol elicits and potentiates nociceptor responses via the vanilloid receptor-1. Nat Neurosci 5:546–551.

Trimmer JS. 2002. Unexpected cross talk: Small GTPase regulation of calcium channel trafficking. Sci STKE E2.

Turner H, Kinet JP. 1999. Signalling through the high-affinity IgE receptor Fc epsilonRI. Nature 402:B24–B30.

Xu H, Ramsey IS, Kotecha SA, Moran MM, Chong JA, Lawson D, Ge P, Lilly J, Silos-Santiago I, Xie Y, DiStefano PS, Curtis R, Clapham DE. 2002. TRPV3 is a calcium-permeable temperature-sensitive cation channel. Nature 418:181–186.